Journal of Power Sources 198 (2012) 95–99

Contents lists available at SciVerse ScienceDirect

Journal of Power Sources

journal homepage: www.elsevier.com/locate/jpowsour

Short communication

Direct ethanol fuel cell: Electrochemical performance at 90 °C on Pt and PtSn/C electrocatalysts

F.L.S. Purgato[a,b], S. Pronier[a], P. Olivi[b], A.R. de Andrade[b], J.M. Léger[a], G. Tremiliosi-Filho[c], K.B. Kokoh[a,*]

[a] Equipe E-lyse, LaCCO-UMR 6503 CNRS, Université de Poitiers, 4 rue Michel Brunet, B27, BP 633, 86022 Poitiers Cedex, France
[b] Departamento de Química da Faculdade de Filosofia, Ciências e Letras de Ribeirão Preto, Universidade de São Paulo, Av. Bandeirantes, 3900, 14040-901 Ribeirão Preto, SP, Brazil
[c] Instituto de Química de São Carlos, Universidade de São Paulo, Caixa Postal 780, 13560-970 São Carlos, SP, Brazil

ARTICLE INFO

Article history:
Received 1 July 2011
Received in revised form
18 September 2011
Accepted 21 September 2011
Available online 29 September 2011

Keywords:
Direct ethanol fuel cell
Ethanol electrooxidation
Pt–Sn
Polymeric precursor method

ABSTRACT

Carbon-supported Pt-based electrocatalysts were synthesized by Pechini method for the ethanol oxidation (EOR). Physicochemical characterizations were helpful to estimate the diameters of the obtained materials ranging from 2 nm to 5 nm. Main electrochemical experiments were carried out at 90 °C *i.e.* under the working conditions of performing the single 5 cm^2 direct ethanol fuel cell (DEFC). $Pt_{80}Sn_{20}/C$ was the anode catalyst which has given the highest power density of 37 mW cm^{-2}. Importantly, the IR spectroscopy measurements associated with the qualitative analysis done at the output of the anodic compartment of the fuel cell have shown that ethanol oxidation on $Pt_{80}Sn_{20}/C$ was mainly a two-electron sustainable process.

1. Introduction

Low temperatures fuel cells such as proton exchange membrane fuel cells (PEMFCs) constitute currently a glimmer of hope in the research of sustainable energy sources. Although anybody does not deny their usefulness to face up the rarefaction of fossil fuels, the finding of active catalysts capable of improving the electrical performances of sustainable-fuel-devices remains an exciting scientific challenge. In this context, we have synthesized by the Pechini method carbon supported Pt based nanoparticles that could be used as anode catalyst for oxidizing ethanol in a direct ethanol fuel cell (DEFC). Our previous contribution [1–9] on the debate related to the role of the co-catalyst [10–34] was helpful because the presence of tin in the composition of the anode catalyst enables to decrease the noble metal amount and supplies surface oxygen-containing-species for the oxidative removal of CO or carbonyl species adsorbed on adjacent Pt active sites. Numerous studies on ethanol electrooxidation have been carried out at room temperature before performing a single DEFC at 80 °C or 90 °C [3,5,6,22,23,34–36]. In the last decade, direct ethanol fuel cell (DEFC) has attracted increasing attention because ethanol has several advantages compared with small organic compounds used as fuels. Recently reflectance infrared spectroscopy measurements have been investigated to determine the reaction products resulted in ethanol oxidation on PtSn anode catalysts [4,6,7,9] Acetaldehyde, acetic acid, CO and CO_2 were identified in different spectra obtained as function of the electrode potential. Furthermore, CO_2 appearance was described as the transformation of a few amount of CO adsorbed at low potential at the surface of platinum. This latter oxidation of CO to CO_2 was easily possible thanks to the presence of tin hydroxide and/or oxide at the platinum surface. This oxidation of ethanol in the bulk solution was confirmed by chromatographic analysis during a long-term amperometric experiment carried out at 0.5 V *vs.* RHE. These investigations have enabled to understand that the ethanol oxidation process led mainly to the two-carbon molecules *i.e.* with a low amount of C–C bond cleavage products [4,7,9]. Importantly PtSn materials may thus be used as anode catalysts in friendly environment devices if one considers that ethanol is produced from biomass (sugar cane, for example). The main focus and challenge are to improve the open circuit voltage of such PEMFCs by diminishing the onset potential of ethanol oxidation and increasing the current densities. For this reason much effort was devoted in the present work to study ethanol electrooxidation at the operating temperature (90 °C) of a 5 cm^2 single DEFC. Although the objective is not herein to analyze the reaction products, a hydrazine solution, indicative of the presence of aldehyde, was put at the output of the fuel cell to observe qualitatively the formation of the major reaction compound.

* Corresponding author. Tel.: +33 549 45 4120; fax: +33 549 45 3580.
E-mail address: boniface.kokoh@univ-poitiers.fr (K.B. Kokoh).

0378-7753/$ – see front matter © 2011 Elsevier B.V. All rights reserved.
doi:10.1016/j.jpowsour.2011.09.060

2. Experimental

2.1. Preparation of the catalysts

The catalysts Pt/C and Pt–Sn/C were synthesized by thermal decomposition of polymeric precursors (DPP). Each metal polymeric precursor was synthesized alone, mixing citric acid (Merck) in ethylene glycol (Merck) at 60–65 °C. After total dissolution of citric acid the temperature was raised to 90 °C and a H_2PtCl_6 solution (in HCl 1:1, v/v) or a tin citrate solution was then added. The citric/ethylene glycol/metal atomic ratios were 16:4:1, respectively, for both platinum and tin solutions. The Pt and Sn precursor solutions were mixed in order to obtain various molar ratios of Pt and Sn (50:50, 60:40, 70:30, 80:20 and 90:10). Sufficient carbon Vulcan XC-72 powder was then added to the mixture in such a quantity to obtain 40 wt% of metal loading. This mixture (precursor solution/carbon) was homogenized in an ultrasonic bath and then heat-treated at different temperatures under an air atmosphere, as previously described [9]. Pt/C catalysts used as reference materials were synthesized under the same conditions.

2.2. Physical characterizations of the materials

The metal-loaded carbon powders were characterized by high resolution transmission electron microscopy (HRTEM) in a JEOL/JEM-3010 microscope operating at 300 kV. The charge of metal loading in the catalyst materials was first determined by Differential Thermal Analysis (DTA)–Thermogravimetric Analysis (TGA). Then an estimation of the elementary particle composition was performed by Energy dispersive X-rays analysis (EDX).

2.3. Electrochemical and analytical measurements

All electrochemical experiments were performed at 90 ± 1 °C under nitrogen atmosphere. The electrolyte solutions were prepared from ultrapure water (Millipore Milli-Q system). Cyclic voltammetry and chronoamperometry measurements were carried out in a conventional three-electrode cell (30 mL) using an Autolab Potentiostat (PGSTAT). As this operating temperature (90 °C) is over the boiling points of ethanol (78.5 °C) and acetaldehyde (20.8 °C) the electrochemical measurements were performed in two times: (i) the supporting electrolyte (0.5 M H_2SO_4) was first deaerated with N_2 gas while the cell was thermostatted at the mentioned temperature; (ii) after adding the organic substrate (0.2 M ethanol) the N_2 flux was stopped to prevent losing any volatile species. At the end of the amperometry measurements, a N_2 gas bubbling was done to carry along the volatile products (especially CO_2) in the gas bubbler which contained 0.1 M NaOH to transform CO_2 to carbonate. The latter ions were easily determined with liquid chromatography (HPLC) equipped with a HPX-87H column and a refractive index detector [9]. A Reversible Hydrogen Electrode (RHE) and a glassy carbon plate with a 4 cm^2 geometric surface area were used as reference and counter electrodes, respectively. Catalysts loadings of 2 mg were used to prepare the anodes. They were dispersed in a solution (500 μL) containing ethanol (475 μL) and Nafion® (25 μL) (5 wt% in aliphatic alcohol, Aldrich). The resulting ink was ultrasonically homogenized for 10 min. After homogenization, a volume of 3 μL was deposited onto vitreous carbon previously polished with alumina (0.5 μm) to a mirror-finish.

2.4. Membrane electrode assembly (MEA) preparation and fuel cell tests

Electrical tests in a single direct ethanol fuel cell were performed using a Globe-Tech test bench. The working conditions such as temperature, pressure, the way to prepare the catalyst and fuel flows are important to obtain the real performance of a system. The membrane electrode assemblies (MEAs) used in the 5 cm^2 single cell tests were prepared by hot pressing a pretreated Nafion® 117 membrane placed between an E-TEK cathode (2 mg cm^{-2} metal loading 40 wt%) and a homemade anode (2 mg cm^{-2} Pt loading 40 wt%) at 130 °C for 3 min, under a pressure of 35 kg cm^{-2}. The operating fuel cell performances were determined in a single DEFC with a geometric surface area of 5 cm^2, using a Globe Tech test bench. The temperature was set to 90 °C for the fuel cell and 95 °C for the oxygen humidifier. The ethanol solution (2 mol L^{-1}) and oxygen pressures were set to 1 and 3 bar, respectively. A wash-flask containing 0.2% of 2,4-dinitrophenylhydrazine in 2 mol L^{-1} acidified hydrazine was placed at the exit of the fuel cell. Its transformation into the corresponding hydrazone (a precipitate) is indicative of the ethanol oxidation to acetaldehyde.

2.5. IR reflectance spectroscopy measurements

IR spectroscopy measurements were performed using a catalyst layer supported on a gold substrate (disk of 7 mm diameter) previously polished with alumina (0.5 μm) to a mirror-finish in order to obtain good reflectivity. The precursor solution was deposited onto the substrate: 5 μL of the catalyst ink, which was prepared from 2 mg of catalyst mixed with 475 μL ethanol and 25 μL Nafion solution. IR reflectance spectra in the wavenumber region 1000–3000 cm^{-1} were collected by a Fourier transform infrared spectrometer (Bruker IFS 66v) with an incidence angle of 65°, after passing through the IR window (CaF_2) of a conventional thin layer spectroelectrochemical cell. This apparatus was equipped with a spectral reflectance device allowing the observation of reflectance spectra of the electrode–electrolyte interface with the IR light beam passing entirely through a chamber under vacuum. This avoids recording parasitic spectra from the air atmosphere. A globar source and a nitrogen cooled mercury–cadmium–telluride (MCT) detector were used. Although the IR experiments were carried out under a conditioned air (25 °C) and the detector was cooled by liquid N_2, we estimate that the spectroscopy measurements are suitable to an investigation at 90 °C since the thin film of the electrolytic solution was certainly heated by the light beam. Data acquisition and processing were performed using a computer with OPUS 5.5 software (developed by Bruker). To apply the technique of Single Potential Alteration Infrared Reflectance Spectroscopy (SPAIRS), the electrode reflectivity R_{Ei} was recorded at different potentials Ei, each separated by 50 mV during the first voltammogram at a sweep rate of 1 mV s^{-1}. Similarly, using the Subtractively Normalized Interfacial Fourier Transform Infrared Reflectance Spectroscopy (SNIFTIRS) method, reflectivities were obtained at two electrode potentials E1 and E2 (the frequency of potential modulation was 25 mHz, and 128 interferograms were collected) and coadded 30 times at each potential. SPAIRS and SNIFTIRS results were displayed as $\Delta R/R = (RE2 - RE1)/RE1 = -\Delta A$, where the "reference" spectrum, RE1, was that recorded at 0.05 V *vs.* RHE for SPAIRS and the amplitude of modulation $\Delta E = E2 - E1$ was maintained constant ($\Delta E = 200$ mV) for SNIFTIRS. If E1 < E2, a positive absorption band indicates the consumption of species and a negative absorption band means the production of species. Both techniques allowed the detection of adsorbed and intermediate species at the electrode surface [4,7].

3. Results and discussion

3.1. Physico-chemical characterization of the electrocatalysts

Without neglecting the other compositions we do the physical characterization of this material as an example (Fig. 1). The dark

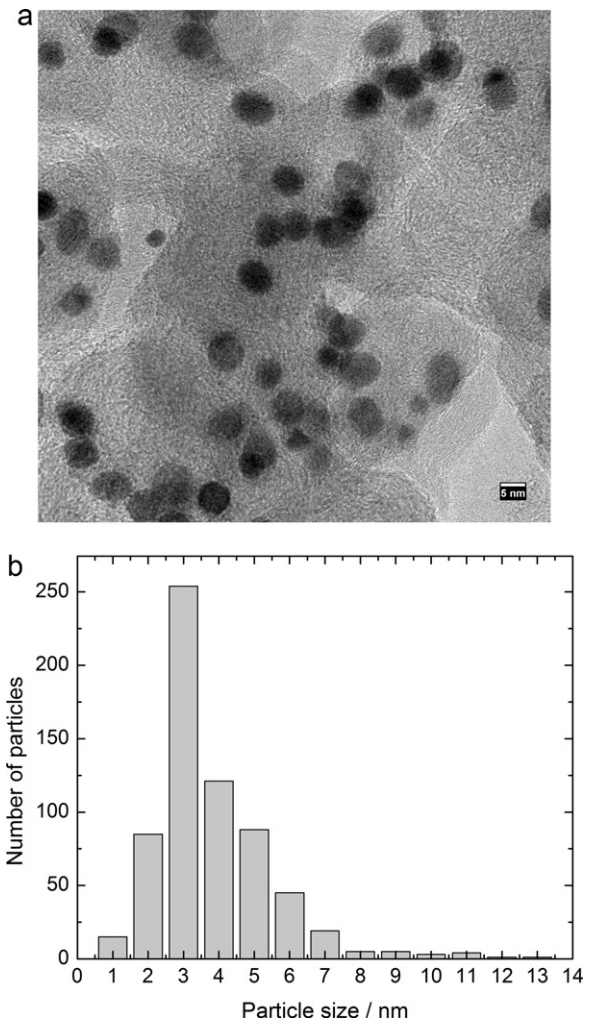

Fig. 1. TEM image and histogram of particle size distribution resulting in the $Pt_{80}Sn_{20}$/C material prepared by the Pechini method.

spots represent the Pt and Sn metals. The TEM image shows that the particle distribution is homogeneous when using the method of thermal decomposition of polymeric metal precursors. The mean catalysts diameter dispersed on Vulcan XC-72 is 3.2 nm. DTA–TGA measurements showed that the metal loading of the material is 40 wt% between 350 °C and 500 °C. The elemental analysis performed by EDX confirmed this nominal composition of $Pt_{80}Sn_{20}$.

3.2. Electrochemical characterization of the catalysts

Fig. 2 shows the cyclic voltammograms of various tin modified Pt-based electrode materials synthesized by the Pechini method. They were recorded at 90 °C which is the operating temperature for measuring the electrical performances of the single DEFC. The current intensities were normalized with the mass of the noble metal (Pt) to take into account the cost of the anode catalyst. It can be seen that the presence of Sn clearly promotes ethanol oxidation because the onset potential on PtSn/C catalysts is at *ca.* 0.3 V *vs.* RHE. This value is centered at 0.5 V *vs.* RHE on Pt/C alone. The effect of temperature is highlighted in Fig. 3 by the comparison of the positive *j*–*E* polarization curves of the $Pt_{80}Sn_{20}$/C composition at 25 °C and 90 °C. Ethanol activation is not only visible with the shift of the onset potential ($\Delta E \approx 300$ mV), but the current densities are higher when increasing the temperature (~14 times at 0.6 V *vs.* RHE).

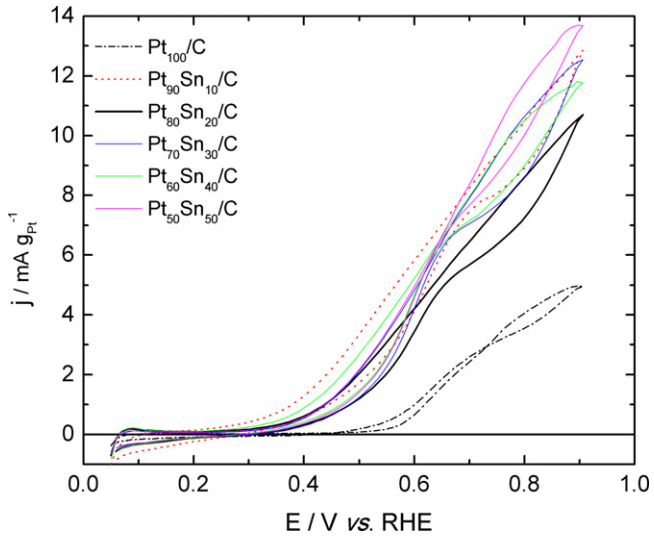

Fig. 2. Voltammograms of Sn modified Pt-based electrode materials recorded at 90 °C and 50 mV s^{-1} in a 0.5 mol L^{-1} H_2SO_4 solution containing 0.2 M ethanol.

It can also be observed that the catalysts containing low tin contents promote ethanol activation at lower potentials. This could be explained by the fact that at low content, Sn decorates the noble metal (Pt) as bimetallic material. Thus, ethanol adsorbs at the Pt sites, while the neighboring Sn sites covered by oxygenated species favor the oxidation of ethanol adsorbates at lower potentials (for example, 0.25 V *vs.* RHE for $Pt_{80}Sn_{20}$/C).

Chronoamperometry measurements were performed at 0.55 V *vs.* RHE to evaluate the catalytic activity of the anode catalysts (Fig. 4). This investigation of the materials in the first minutes at 90 °C permits to estimate their stability under the working conditions. During the first seconds, there is a sharp decrease in the current density followed by a slow decrease in the current values for longer time periods and a steady-state current is observed for all studied catalysts after *ca.* 200 s. As can be seen in the figure, and conversely to the previous statement concerning the low tin content in the catalyst compositions it is worthy of note that $Pt_{70}Sn_{30}$/C and $Pt_{80}Sn_{20}$/C electrodes have a better electrocatalytic activity and stability towards ethanol oxidation. This efficiency could result in their composition which is a mixture of alloyed and bimetallic forms [6,9]. On the one side the Pt_3Sn structure is well-known to promote ethanol oxidation to acetaldehyde at low

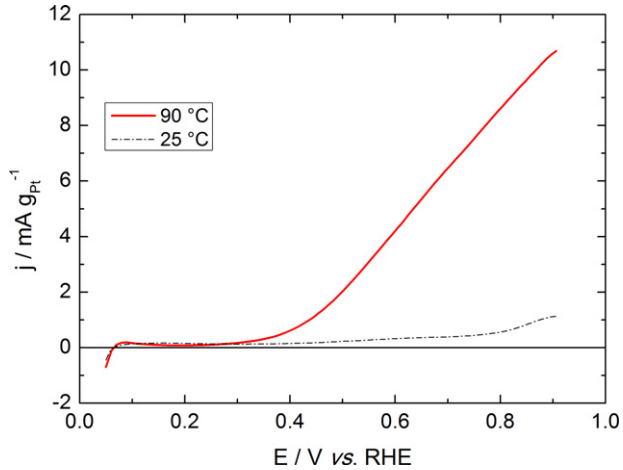

Fig. 3. Positive potential scans of a $Pt_{80}Sn_{20}$/C electrode material recorded at 25 °C and 90 °C in 0.5 mol L^{-1} H_2SO_4 containing 0.2 mol L^{-1} ethanol with a scan rate of 50 mV s^{-1}.

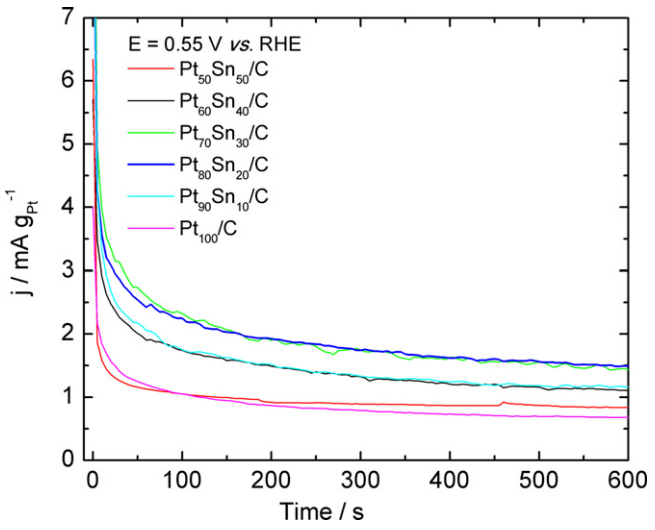

Fig. 4. Current *vs.* time plots for the oxidation of 0.2 mol L^{-1} ethanol in 0.5 mol L^{-1} H_2SO_4 at 0.55 V *vs.* RHE and 90 °C on various Pt–Sn/C anode catalysts compositions. Current values were normalized with the Pt content.

potentials (alloying effect) [26,33,35,37–41]. On the other hand, the tin content at the vicinity of the Pt sites in the bimetallic composition does contribute to a bifunctional reaction process favoring oxygenated-donor effect on the removal of the adsorbed species at the Pt surface and the contribution to the formation of acetic acid [5,6,13,17,21,23,25,27]. At the end of the amperometric experiments the bulk solution was injected in liquid chromatography. The analytes are mainly acetaldehyde and acetic acid in low concentration. Additionally, nitrogen was bubbled in the cell to carry along the volatile compounds in the gas bubbler. The chromatographic analysis of its content showed that NaOH has trapped CO_2 and acetaldehyde. Table 1 summarizes the profile of the reaction products resulted in the ethanol oxidation on the PtSn anode catalysts at 0.55 V *vs.* RHE.

3.3. Spectroelectrochemical characterization of the catalysts

Infrared reflectance spectroscopy characterizations of the PtSn anode catalysts were recently obtained [9]. We confirm herein the determination of some intermediates which are necessary to evaluate the efficiency of these materials synthesized towards the ethanol oxidation. Therefore, SPAIRS and SNIFTIRS techniques were performed in a 0.5 mol L^{-1} H_2SO_4 solution containing 0.2 mol L^{-1} ethanol (Fig. 5). Acetaldehye, acetic acid, CO and CO_2 are the different species determined as issued from the ethanol oxidation on the synthesized catalysts. As the band centered at 1712 cm^{-1} can be attributed to the stretching mode (ν_{CO}) of acetaldehyde (CHO) and acetic acid (COOH), we focused the ascription of the

Table 1
Distribution of the reaction products formed during the ethanol oxidation at 90 °C on $Pt_{80}Sn_{20}$/C anode catalyst.

Reaction products	FTIR	HPLC
CO	2050 cm^{-1} (linearly bonded)	[a]
CO_2	2345 cm^{-1} (C–O asymmetric stretching)	1.7 mM
Acetaldehyde	1712 cm^{-1} (C=O stretching of CHO)	12.3 mM
Acetic acid	1258 cm^{-1} (C–O stretch vibration) 1420 cm^{-1} (adsorbed CH_3COO^-: C–O symmetric stretching) 1712 cm^{-1} (C=O stretching of COOH)	Traces (0.1 mM)

[a] Not observed.

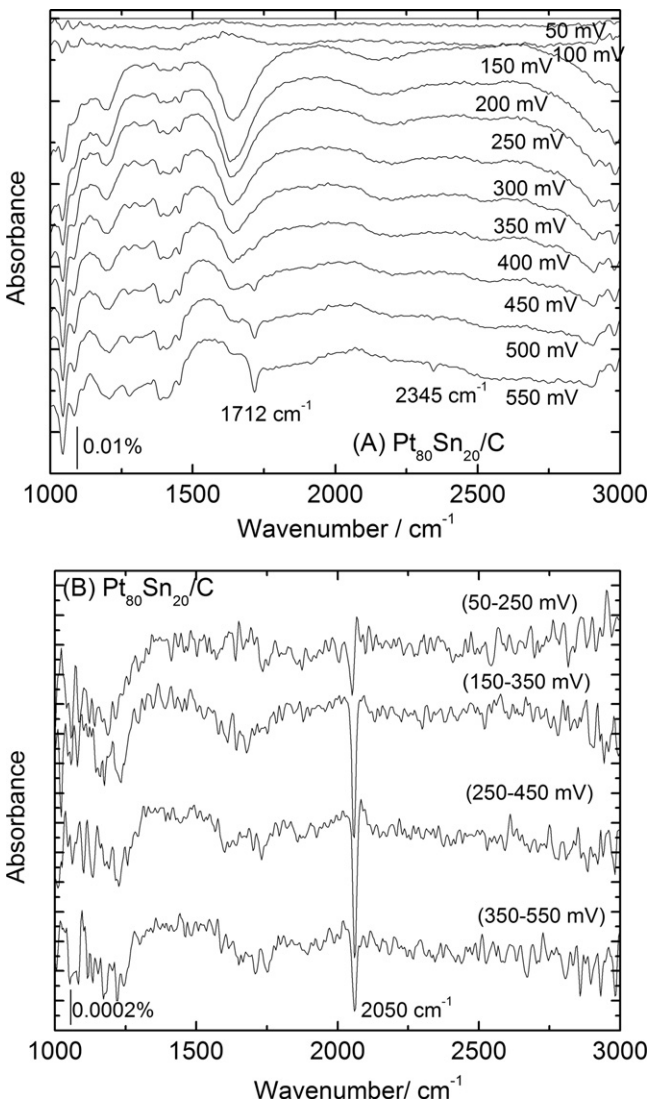

Fig. 5. (A) SPAIR spectra of the species resulting in adsorption and oxidation of 0.2 mol L^{-1} ethanol in 0.5 mol L^{-1} H_2SO_4 on a $Pt_{80}Sn_{20}$/C electrode at different potentials varying from 50 mV to 550 mV *vs.* RHE. R_{ERef} was taken at 50 mV. (B) SNIFTIR spectra of the species coming from ethanol adsorption and oxidation on $Pt_{80}Sn_{20}$/C electrode. 0.2 mol L^{-1} ethanol; T = 25 °C at various potential modulations from 50 mV to 550 mV *vs.* RHE.

adsorbed species with other bands. Indeed, the bands localized at 1280 cm^{-1} and 1417 cm^{-1} due to C–O stretch vibration and the C–O symmetric stretching (adsorbed CH_3COO^-), respectively, can be assigned to the formation of acetic acid [41]. The presence of the later product as the main reaction product would provide a broad band due to the O–H stretching of COOH at 2615–2630 cm^{-1} [42]. Importantly, CO_L and CO_2 are also present in the spectra at 2050 cm^{-1} and 2345 cm^{-1}, respectively (Table 1). Their presence is undoubtedly indicative of the cleavage of the C–C bond. But it is also worthy of note that the cleavage molecules are in small amounts. This provides evidence that the Sn content in the catalyst composition promotes the Pt material according to a bifunctional mechanism.

3.4. Catalysts activity in a single fuel cell

The performances of the various Pt-based catalysts synthesized for the anode event of a 5 cm^2 single DEFC are shown in Fig. 6.

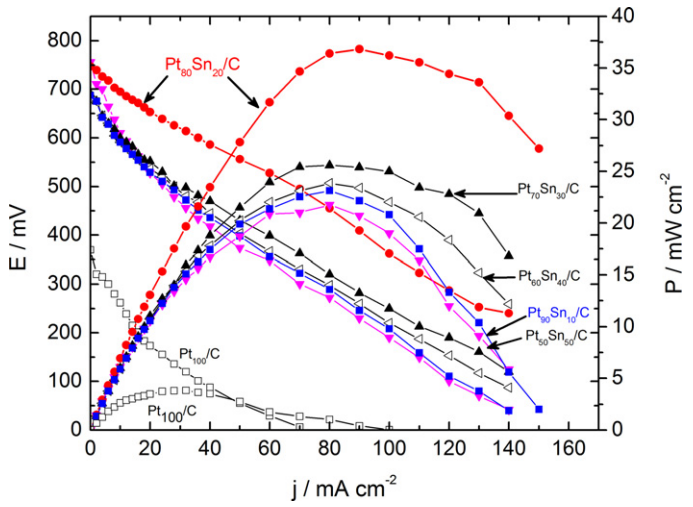

Fig. 6. Performances of a 5 cm^2 single direct ethanol fuel cell recorded at 90 °C using various tin modified Pt-based anodes (2 mg cm^{-2} catalyst loading, 40 wt% catalyst on Vulcan XC-72); cathode catalyst: 2 mg cm^{-2} (Pt/C, 40 wt% from E-TEK); membrane: Nafion® 117; ethanol concentration: 2.0 mol L^{-1}; p_{EtOH} = 1 bar; p_{O_2} = 3 bar.

The efficiency of the better anode ($Pt_{80}Sn_{20}$/C) is in line with the chronoamperometry measurements. The open circuit voltage (OCV) is of 750 mV and the power density with this catalyst composition reaches 37 mW cm^{-2} at 90 mA cm^{-2}. However, it should be noted that the power density obtained herein with Pt/C is lower than that regularly found in the literature close to 10–12 mW cm^{-2} [6,23].

At the output of the anodic compartment of the cell the phenylhydrazine formed a precipitate indicative of the presence of a corresponding hydrazone which is synonym of the production of acetaldehyde. The combination of this result with that of IR spectroscopy enables to state that acetaldehyde is the main reaction molecule produced by the DEFC on $Pt_{80}Sn_{20}$/C anode. This means that the oxidation process involves mainly two electrons. Although it is a weak Faradaic yield, it remains a promising system because it delivers a suitable power density and importantly provides a C2-molecule as reaction product.

4. Conclusion

Tin modified Pt-based anode catalysts were synthesized by the method of Thermal Decomposition of Polymeric metal precursors (DPP). This process has enabled to control the heat-treatment which is the preparation stage to obtain an expected size distribution of nanoparticles. Acetaldehyde was determined as the main reaction product. This two-electron reaction process first shows that $Pt_{80}Sn_{20}$/C anode can dehydrogenate ethanol at low potential regarding the appearance of the band centered at 1712 cm^{-1}. Furthermore, the steady-state oxidation currents observed could be interpreted as a bifunctional mechanism likely due to the presence of oxygenated species of Sn oxides and/or hydroxides which are helpful to remove intermediates issued from the dissociative ethanol adsorption. On the other side, the catalyst composition probably contains a Pt_3Sn phase which activates interfacial water. Ethanol oxidation at *ca.* 0.3 V *vs.* RHE requires such neighboring hydroxyl species to transform the small amount of adsorbed CO into CO_2. This removal of the catalyst surface is useful to maintain the electrical performance of the fuel cell which in this case is a promising sustainable device.

Acknowledgements

This work was mainly conducted within the framework of a collaborative program CAPES/COFECUB under grant n°498/05. F.L.S. Purgato acknowledges CAPES for the postdoctoral fellowship (BEX n°0509078).

References

[1] D.M. Dos Anjos, K.B. Kokoh, J.M. Leger, A.R. De Andrade, P. Olivi, G. Tremiliosi, J. Appl. Electrochem. 36 (2006) 1391–1397.
[2] R. Sousa Jr., D.M. dos Anjos, G. Tremiliosi-Filho, E.R. Gonzalez, C. Coutanceau, E. Sibert, J.-M. Léger, K.B. Kokoh, J. Power Sources 180 (2008) 283–293.
[3] J. Ribeiro, D. dos Anjos, J. Léger, F. Hahn, P. Olivi, A. de Andrade, G. Tremiliosi-Filho, K. Kokoh, J. Appl. Electrochem. 38 (2008) 653–662.
[4] D.M. dos Anjos, F. Hahn, J.M. Leger, K.B. Kokoh, G. Tremiliosi, J. Braz. Chem. Soc. 19 (2008) 795–802.
[5] F.C. Simões, D.M. dos Anjos, F. Vigier, J.M. Léger, F. Hahn, C. Coutanceau, E.R. Gonzalez, G. Tremiliosi-Filho, A.R. de Andrade, P. Olivi, K.B. Kokoh, J. Power Sources 167 (2007) 1–10.
[6] J. Ribeiro, D.M. dos Anjos, K.B. Kokoh, C. Coutanceau, J.M. Léger, P. Olivi, A.R. de Andrade, G. Tremiliosi-Filho, Acta Electrochim. 52 (2007) 6997–7006.
[7] D. dos Anjos, F. Hahn, J.M. Léger, K. Kokoh, G. Tremiliosi-Filho, J. Solid State Electrochem. 11 (2007) 1567–1573.
[8] T.S. Almeida, K.B. Kokoh, A.R. De Andrade, Int. J. Hydrogen Energy 36 (2011) 3803–3810.
[9] F.L.S. Purgato, P. Olivi, J.M. Léger, A.R. de Andrade, G. Tremiliosi-Filho, E.R. Gonzalez, C. Lamy, K.B. Kokoh, J. Electroanal. Chem. 628 (2009) 81–89.
[10] M. Zhu, G. Sun, S. Yan, H. Li, Q. Xin, Energy Fuels 23 (2008) 403–407.
[11] Q. Yi, J. Zhang, A. Chen, X. Liu, G. Xu, Z. Zhou, J. Appl. Electrochem. 38 (2008) 695–701.
[12] E.V. Spinacé, L.A. Farias, M. Linardi, A.O. Neto, Mater. Lett. 62 (2008) 2099–2102.
[13] A.O. Neto, L.A. Farias, R.R. Dias, M. Brandalise, M. Linardi, E.V. Spinacé, Electrochem. Commun. 10 (2008) 1315–1317.
[14] A.O. Neto, R.R. Dias, M.M. Tusi, M. Linardi, E.V. Spinacé, J. Power Sources 166 (2007) 87–91.
[15] E.V. Spinacé, M. Linardi, A.O. Neto, Electrochem. Commun. 7 (2005) 365–369.
[16] E. Ribadeneira, B.A. Hoyos, J. Power Sources 180 (2008) 238–242.
[17] Y. Guo, Y. Zheng, M. Huang, Electrochim. Acta 53 (2008) 3102–3108.
[18] A. Bonesi, G. Garaventa, W.E. Triaca, A.M. Castro Luna, Int. J. Hydrogen Energy 33 (2008) 3499–3501.
[19] J.C. Bauer, X. Chen, Q. Liu, T.-H. Phan, R.E. Schaak, J. Mater. Chem. 18 (2008) 275–282.
[20] G. Wu, R. Swaidan, G. Cui, J. Power Sources 172 (2007) 180–188.
[21] P.E. Tsiakaras, J. Power Sources 171 (2007) 107–112.
[22] H. Li, G. Sun, L. Cao, L. Jiang, Q. Xin, Electrochim. Acta 52 (2007) 6622–6629.
[23] L. Jiang, L. Colmenares, Z. Jusys, G.Q. Sun, R.J. Behm, Electrochim. Acta 53 (2007) 377–389.
[24] R. Chetty, K. Scott, Electrochim. Acta 52 (2007) 4073–4081.
[25] Z. Liu, B. Guo, L. Hong, T.H. Lim, Electrochem. Commun. 8 (2006) 83–90.
[26] F. Colmati, E. Antolini, E.R. Gonzalez, J. Power Sources 157 (2006) 98–103.
[27] L. Jiang, G. Sun, Z. Zhou, S. Sun, Q. Wang, S. Yan, H. Li, J. Tian, J. Guo, B. Zhou, Q. Xin, J. Phys. Chem. B 109 (2005) 8774–8778.
[28] L. Jiang, G. Sun, S. Wang, G. Wang, Q. Xin, Z. Zhou, B. Zhou, Electrochem. Commun. 7 (2005) 663–668.
[29] L. Jiang, G. Sun, S. Sun, J. Liu, S. Tang, H. Li, B. Zhou, Q. Xin, Electrochim. Acta 50 (2005) 5384–5389.
[30] W.J. Zhou, B. Zhou, W.Z. Li, Z.H. Zhou, S.Q. Song, G.Q. Sun, Q. Xin, S. Douvartzides, M. Goula, P. Tsiakaras, J. Power Sources 126 (2004) 16–22.
[31] F. Vigier, C. Coutanceau, A. Perrard, E.M. Belgsir, C. Lamy, J. Appl. Electrochem. 34 (2004) 439–446.
[32] F. Vigier, C. Coutanceau, F. Hahn, E.M. Belgsir, C. Lamy, J. Electroanal. Chem. 563 (2004) 81–89.
[33] L. Jiang, Z. Zhou, W. Li, W. Zhou, S. Song, H. Li, G. Sun, Q. Xin, Energy Fuels 18 (2004) 866–871.
[34] W. Zhou, Z. Zhou, S. Song, W. Li, G. Sun, P. Tsiakaras, Q. Xin, Appl. Catal. B: Environ. 46 (2003) 273–285.
[35] Q. Wang, G.Q. Sun, L. Cao, L.H. Jiang, G.X. Wang, S.L. Wang, S.H. Yang, Q. Xin, J. Power Sources 177 (2008) 142–147.
[36] W.J. Zhou, W.Z. Li, S.Q. Song, Z.H. Zhou, L.H. Jiang, G.Q. Sun, Q. Xin, K. Poulianitis, S. Kontou, P. Tsiakaras, J. Power Sources 131 (2004) 217–223.
[37] A.V. Tripkovic, K.D. Popovic, J.D. Lovic, V.M. Jovanovic, S.I. Stevanovic, D.V. Tripkovic, A. Kowal, Electrochem. Commun. 11 (2009) 1030–1033.
[38] H. Wang, Z. Jusys, R.J. Behm, J. Power Sources 154 (2006) 351–359.
[39] L. Colmenares, H. Wang, Z. Jusys, L. Jiang, S. Yan, G.Q. Sun, R.J. Behm, Electrochim. Acta 52 (2006) 221–233.
[40] P. Liu, A. Logadottir, J.K. Nørskov, Electrochim. Acta 48 (2003) 3731–3742.
[41] S. García-Rodríguez, S. Rojas, M.A. Peña, J.L.G. Fierro, S. Baranton, J.M. Léger, Appl. Catal. B: Environ. 106 (2011) 520–528.
[42] T. Iwasita, F.C. Nart, Prog. Surf. Sci. 55 (1997) 271–340.